HIGHLY SELECTIVE H₂ SEPARATION ZEOLITE MEMBRANES FOR COAL GASIFICATION MEMBRANE REACTOR APPLICATIONS

Annual Technical Progress Report

Reporting Period:

September 2005 – September 2006

DOE Award No. DE-FG26-02NT41536

Mei Hong (student), Richard D. Noble[*] (PI), and John L. Falconer (co-PI)

University of Colorado at Boulder

Department of Chemical and Biological Engineering

Boulder, Colorado 80309-0424

Phone: (303) 492 6100; Fax: (303) 492 4341; Email: Nobler@Colorado.edu

February 8, 2007

DISCLAIMER

ABSTRACT

Zeolite membranes are thermally, chemically, and mechanically stable. They also have tunable molecular sieving and catalytic ability. These unique properties make zeolite membrane an excellent candidate for use in catalytic membrane reactor applications related to coal conversion and gasification, which need high temperature and high pressure range separation in chemically challenging environment where existing technologies are inefficient or unable to operate. Small pore, good quality, and thin zeolite membranes are needed for highly selective H_2 separation from other light gases (CO_2, CH_4, CO). However, zeolite membranes have not been successful for H_2 separation from light gases because the zeolite pores are either too big or the membranes have a large number of defects. The objective of this study is to develop zeolite membranes that are more suitable for H_2 separation.

In an effort to tune the size of zeolite pores and/or to decrease the number of defects, medium-pore zeolite B-ZSM-5 (MFI) membranes were synthesized and silylated. Silylation on B-ZSM-5 crystals reduced MFI-zeolite pore volume, but had little effect on CO_2 and CH_4 adsorption. Silylation on B-ZSM-5 membranes increased H_2 selectivity both in single component and in mixtures with CO_2, CH_4, or N_2. Single gas and binary mixtures of H_2/CO_2 and H_2/CH_4 were separated through silylated B-ZSM-5 membranes at feed pressures up to 1.7 MPa and temperatures up to 773 K. For one B-ZSM-5 membrane after silylation, the H_2/CO_2 separation selectivity at 473 K increased from 1.4 to 37, whereas the H_2/CH_4 separation selectivity increased from 1.6 to 33. Hydrogen permeance through a silylated B-ZSM-5 membrane was activated, but the CO_2 and CH_4 permeances decreased slightly with temperature in both single gas and in mixtures. Therefore, the H_2 permeance and H_2/CO_2 and H_2/CH_4 separation selectivities increased with temperature. At 673 K, the H_2 permeance was 1.0×10^{-7} mol·m^{-2}·s^{-1}·Pa^{-1}, and the H_2/CO_2 separation selectivity was 47. Above 673 K, the silylated membrane catalyzed reverse water gas shift reaction and still separated H_2 with high selectivity; and it was thermally stable. However, silylation decreased H_2 permeance more than one order of magnitude. The H_2 separation performance of the silylated B-ZSM-5 membranes depended on the initial membrane quality and acidity, as well as the silane precursors. Increasing the membrane feed pressure also increased the H_2 flux and the H_2 mole fraction in the permeate stream for both mixtures.

Another approach used in this study is optimizing the synthesis of small-pore SAPO-34 (CHA) membranes and/or modifying SAPO-34 membranes by silylation or ion exchange. For SAPO-34 membranes, strong CO_2 adsorption inhibited H_2 adsorption and decreased H_2 permeances, especially at low temperatures. At 253 K, CO_2/H_2 separation selectivities of a SAPO-34 membrane were greater than 100 with CO_2 permeances of about 3×10^{-8} mol·m^{-2}·s^{-1}·Pa^{-1}. The high reverse-selectivity of the SAPO-34 membranes can minimize H_2 recompression because H_2 remained in the retentate stream at a higher pressure. The CO_2/H_2 separation selectivity exhibited a maximum with CO_2 feed concentration possibly caused by a maximum in the CO_2/H_2 sorption selectivity with increased CO_2 partial pressure. The SAPO-34 membrane separated H_2 from CH_4 because CH_4 is close to the SAPO-34 pore size so its diffusivity is much lower than the H_2

diffusivity. The H_2/CH_4 separation selectivity was almost independent of temperature, pressure, and feed composition. Silylation on SAPO-34 membranes increased H_2/CH_4 and CO_2/CH_4 selectivities but did not increase H_2/CO_2 and H_2/N_2 selectivities because silylation only blocked defects in SAPO-34 membranes. Hydrogen cations in SAPO-34 membranes were exchanged with Li^+, Na^+, K^+, NH_4^+, and Cu^{2+} cations in non-aqueous solutions in an effort to improve their gas separation performance. H-SAPO-34 crystals were exchanged under the same conditions and their adsorption properties were measured. Ion exchange with Cu^{2+} increased CO_2 adsorption strength, whereas Li^+ exchange decreased the SAPO-34 pore volume and saturation loadings of CO_2 and CH_4. Ideal and separation selectivities for H_2/CH_4 mixtures increased less than 18%, whereas ideal and separation selectivities for CO_2/CH_4 mixtures increased up to 60% due to ion exchange of zeolite membranes. Gas permeances decreased upon ion exchange, and the decrease was larger for large cations, apparently due to steric hindrance. Multiple exchanges did not degrade SAPO-34 crystals or membranes.

This is the fourth annual technical progress report for the university coal research program supported by U.S. DOE NETL (Contract No. DE-FG26-02NT41536). This report summarizes program accomplishments up to September 2006. The report includes an introduction summarizing the research objectives and tasks; it also provides a summary of program activities and accomplishments covering progress in various zeolite membrane synthesis and modification; the membranes had high permeances and selectivities exceeding the upper bounds of polymer membranes. Possible future work is proposed as well.

TABLE OF CONTENTS

LIST OF FIGURES

LIST OF TABLES

1. INTRODUCTION

Hydrogen is a clean energy source and is in increasing demand in petroleum refining and petrochemical production. Hydrogen can be produced from coal conversion and gasification process where coal is converted into synthesis gas. Depending on the particular gasification process, the synthesis gas produced also contains carbon dioxide, methane, carbon monoxide, hydrogen sulfide, water, and other gases. Hydrogen recovery from coal gasification products requires an efficient separation process to purify the gas economically. Most H_2 is separated by pressure-swing amine adsorption, but these plants suffer from serious operational drawbacks, including equipment corrosion, complex operation, material loss, personnel safety, and environmental impact. Membrane separation is an attractive alternative because of its ease of operation, low energy consumption, and cost effectiveness even at low gas volumes. Most membranes for H_2 separation preferentially permeate H_2, which is produced on the permeate side at low pressures, and it must then be recompressed at significant energy cost. Reverse-selective membranes, i.e., membranes that preferentially remove large permeating molecules from small ones in the mixture, can minimize H_2 recompression because H_2 is in the retentate stream at a higher pressure. Among various membrane materials, zeolite membranes attract more and more attention because of their molecular-sized pores and their high thermal, chemical, and mechanical stability.

Zeolites are microporous crystalline alumino-silicates, with uniform pores in the molecular size range; the pore size distribution is extremely narrow. Most zeolites contain Si and Al, but other metals (B, Fe, and Ge) can be isomorphously substituted in some framework instead of Al and some frameworks can be prepared in the pure Si form. Among various types of zeolite membranes synthesized to date, ten-member ring MFI structure (silicalite-1 and ZSM-5) is the most extensively studied case. MFI-type membranes have straight, circular channels of 0.54×0.56 nm running perpendicular to sinusoidal, elliptical channels of 0.51×0.54 nm, and are suitable for separations of several industrially important organic molecules. When B substitutes Al in the framework of MFI structure, it is called B-ZSM-5 zeolite. Light gas including H_2 separations through MFI membranes are often dominated by competitive adsorption, rather than size exclusion because the MFI pore size is much bigger than the size of light gases. The as-synthesized MFI membranes are sometimes selective towards CO_2 and CH_4, although H_2 is the smallest molecule because the adsorption of CO_2 and CH_4 is stronger than that of H_2, especially at low temperatures. Small pore zeolite membranes have been synthesized, which include zeolite A, SAPO-34, ETS-4, SSZ-13 and sodalite membranes. Our group has successfully synthesized SAPO-34 membranes. The SAPO-34 is a silicoaluminophosphate and its structure is a chabazite analog, which have 8-member ring CHA structure with pore size of 0.38 nm. The membranes showed high CO_2/CH_4 selectivities at low temperature range, but still have bigger non-zeolite defects in the structure.

Inorganic zeolite membranes have the ability to operate the separation at or near the processing conditions for H_2 production. They can tolerate high temperatures, high pressure-drops and chemically challenging environments. A zeolite layer can be

fabricated onto a tubular support, providing high surface to volume ratio, scale up in modular form and the ability to continuously separate. Moreover, zeolites have catalytic properties, which make it possible to integrate reaction and separation into one unit. In zeolite materials, hydrogen has a higher diffusivity than most molecules, but it adsorbs weakly, so that diffusion favors H_2 permeation but competitive adsorption favors permeation of other molecules. One challenge for H_2 separation is that H_2 (0.289 nm) differs less than 0.1 nm in kinetic diameter from H_2O (0.265 nm), CO_2 (0.33 nm), CO (0.376 nm), and CH_4 (0.38 nm). To selectively separate H_2 from other light gases (CO, CO_2, CH_4), the zeolite membrane will have to discriminate between molecules that are approximately 0.3-0.4 nm in size and 0.1 nm or less in size difference. The zeolite membranes need to have small pores and negligible amount of defects to ensure high selectivity. They also need to be thin to ensure high flux. Due to the difficulty in making good-quality, small-pore zeolite membranes, only a few studies have reported H_2 separation through zeolite membranes; most reported only ideal selectivities. Most zeolite membranes have not been successful for H_2 separation because the as-synthesized zeolite membranes either have zeolite pores too big for separating H_2 from other light gases and/or have many non-zeolite pores bigger than the zeolite pores, so called defects. Zeolite membranes with smaller pores have the potential to effectively separate H_2 from other light gases, if they are made defect-free. To accomplish this goal, we can either synthesize small-pore zeolite membranes that have pores in this size range, or post-treat existing zeolite membranes to systematically reduce the pore size and/or the number of defects so as to create good-quality zeolite membranes with desirable pore diameters suitable for hydrogen separation.

For this project, we synthesized medium-pore B-ZSM-5 membranes and small-pore SAPO-34 membranes. Some as-synthesized zeolite membranes were post-treated to post-treat to alter their zeolite pore size and defects size. The post treatment methods include silylation and ion exchange. In the silylation reaction, silane precursor was firstly chemisorbed onto the acid sites within the zeolite membrane, then catalytically cracked on sites and oxidized. As a result, additional silicon atoms were added to the original zeolite structures, and the effective pore opening size of the defects and/or zeolite pores was decreased. In the ion exchange reaction, part of H^+ ions in the zeolite membranes was replaced by other metal cations. As a result, zeolite adsorption and/or diffusion properties changed, causing changes of the membrane permeation and separation properties. The effects of initial membrane properties and the modification parameters were studied in detail. The effect of separating conditions, such as temperature, pressure, and feed compositions, have been analyzed. Single gas H_2, CO_2, and CH_4 permeations have been measured for comparison. Zeolite crystals have been synthesized and post-treated the same way and the crystal adsorption and pore volume changes have been investigated.

2. EXPERIMENTAL METHODS

2.1 Zeolite membrane synthesis

2.1.1 B-ZSM-5 membranes

Some B-ZSM-5 membranes (B1-B4) were prepared by secondary growth on the inner surface of porous (200-nm pores in inner layer; 0.35 porosity), tubular, asymmetric α-alumina supports (Pall Corporation). Silicalite-1 seeds of ~ 100 nm were made from a gel with a molar composition of 9 TPAOH: 24 TEOS: 500 H_2O. The template, tetra-propyl ammonium hydroxide (TPAOH, 1.0 M aqueous solution, Aldrich), was added drop wise into tetraethoxysilane (TEOS, 98+%, Aldrich) with strong agitation. The solution was aged for 1-3 days at room temperature, and then crystals were grown at 358 K with constant stirring at 250 rpm for 3 days. The seeds were washed and dispersed into deionized water to form a stable 2 wt% colloidal suspension. The α-alumina supports were dip-coated in the silicalite-1 seed suspension for 5 min and dried in a 373 K vacuum oven for 20 min. The dip-coating procedure was repeated three times. The secondary growth gel had a molar composition of 16 TPAOH: 80 TEOS : 6.5 $B(OH)_3$: 5000 H_2O with a Si/B ratio of 12.5. In an attempt to minimize penetration into the support, the gel viscosity was increased by adding 2 wt% surfactant cetyltrimethyl ammonium bromide (Aldrich) to the gel after the gel was aged for a day. Crystallization was carried out at 458 K for 4 h in a horizontal autoclave that was continuously rotated. An additional layer was applied using the same procedure, and the membranes were prepared with two layers. The membranes were impermeable to N_2 for a 138-kPa pressure drop at room temperature and were calcined in air at 753 K for 8 h with a heating and cooling rate of 0.6 and 1.1 K/min respectively to remove the TPAOH template from the framework. The B-ZSM-5 crystals were also synthesized from the silicalite-1 seeds by secondary growth, using the same procedure as for membrane synthesis.

The synthesis methods for other MFI-type membranes, such as B-ZSM-5 (Si/B=100 in the gel, B4) and silicalite-1 (Si/B=infinity in the gel, B5) membranes, have been reported in our previous reports (Table 1).

2.1.2 SAPO-34 membranes

Some SAPO-34 membranes (S1-S8, S11-12) were prepared by in-situ crystallization onto tubular stainless steel supports (0.8-μm pores, Pall Corp.). Non-porous, stainless steel tubes were welded onto each end of the support to provide nonporous surfaces for sealing the membranes in the module. The permeate area was 7.8 cm^2. The synthesis gel had a molar composition of Al_2O_3 : P_2O_5: 0.6 SiO_2: 1.07 TEAOH: 56 H_2O with a Si/Al ratio of 0.3. The gel was prepared by stirring H_3PO_4 (85 wt% aqueous solution), $Al(i-C_3H_7O)_3$, and H_2O at room temperature for 12 h. The template, tetra-ethyl ammonium hydroxide (TEAOH, 35 wt% aqueous solution), was then added and the mixture was stirred for 30 min before the colloidal silica sol (Ludox AS40) was added. The porous stainless steel support, with its outside wrapped in Teflon tape, was placed in an autoclave with synthesis gel both inside and outside the support tube. The hydrothermal synthesis was carried out at 468 K for 20 h. After synthesis, the membrane was washed with distilled water at room temperature and dried at 373 K in a vacuum oven for 2 h. Additional layers were applied using the same procedure, and membranes were prepared with 4 layers. The SAPO-34 membranes were calcined in air at 663 K for

20 h with heating and cooling rates of 0.6 and 0.9 K/min respectively and stored in a 373 K oven until usage. The SAPO-34 crystals were also synthesized using the same gel, synthesis temperature, and time.

Two SAPO-34 membranes (S9-10) were synthesized from a gel that had a molar composition of Al_2O_3: P_2O_5: 0.3 SiO_2: 1.2 TEAOH: 55 H_2O with a Si/Al ratio of 0.15. The hydrothermal synthesis was carried out at 473 K for 24 h. After synthesis, the membranes were washed with distilled water at room temperature and dried at 373 K in a vacuum oven for 2 h. Additional layers were applied using the same procedure, and membrane was prepared with 4 layers. The SAPO-34 membranes were calcined in air at 663 K for 20 h, with a heating and cooling rate of 0.6 and 0.9 K/min, respectively, and they were stored in a ~500 K oven.

2.2 Silylation on zeolite membranes

For silylation with methyldiethoxysilane (MDES), the zeolite membranes were first outgassed in N_2 (UHP grade, Airgas) flow at 623 K overnight. Then N_2 bubbled through liquid methyldiethoxysilane (97+%, Alfa Aesar) at 297 K and flowed through the inside of the membrane tubes at 623 K for 10 h. After that, the membrane inside was then flushed with N_2, heated to 823 K with a heating rate of 0.6 K/min in air (breathing quality, Airgas) for 4 h, and cooled down in flowing N_2 at a rate of 1.1 K/min. The outgas-silylation-calcination cycle was repeated once. The same silylation procedures were used for SAPO-34 membranes except that the oxidation step was at 663 K and the oxidation time was extended to about 20 h.

For silylation of a B-ZSM-5 membrane with silane (SiH_4), the membrane was first outgassed in N_2 flow at 623 K overnight and cooled to 473 K with a heating and cooling rate of 0.6 and 1.1 K/min respectively. Dilute silane (0.8% SiH_4 in N_2, Airgas) flowed through the inside of the membrane tube at 473 K for 40 h. After the silane flow was shut off, N_2 gas bubbled through a water reservoir at 297 K to oxidize the membrane tube at 473 K for 20 h. The membrane was then flushed with N_2 at 473 K for 20 h to remove any physically adsorbed water. This silylation-oxidation-dehydration cycle was repeated once. Table 1 shows the synthesis and silylation conditions of different MFI membranes discussed in this report.

Table 1 Synthesis and silylation conditions for B-ZSM-5 membranes

Membrane Number	Zeolite Type	Synthesis Method	Si/B ratio	Silane precursor
B1-B3	B-ZSM-5	Secondary growth	12.5	MDES
B4	B-ZSM-5	Secondary growth	12.5	Silane
B5	B-ZSM-5	I n-situ cystallization	100	MDES
B6	Silicalite-1	In-situ crystallization	Infinity	MDES

2.3 Ion exchange on SAPO-34 membranes

The as-synthesized SAPO-34 membranes have negatively charged framework structure, and H^+ ions were present in the extra framework for charge neutralization. The H^+ ions in the SAPO-34 membranes were exchanged with bigger metal cations. The acetate salts (Aldrich) of Li^+ (99.99%), Na^+ (99+%), K^+ (99+%), NH_4^+ (99.999%), and Cu^{2+} (monohydrate, 98+%) were dissolved in ethanol for ion exchange solutions. Each membrane was tied to a magnetic stirrer with Teflon tape and placed at the bottom of a flask that had a reflux system and contained an ion exchange solution. The membranes were stirred at ~100 rpm in 150 mL of the exchange solution at 348 K for 4 h. Membrane S7 was exchanged at slightly different conditions: 328 K and methanol solvent. After exchange, the membranes were washed three times with ~100 mL ethanol while stirring at ~100 rpm for at least 30 min each time. They were then dried at 340 K under vacuum for 2 h and further dried at 473 K overnight. The exchange process was repeated at the same or different conditions for some membranes (Table 2).

Table 2 Ion exchange conditions for SAPO-34 membranes

Membrane	Precursor ions		Ion concentration (M)		
	Ion	Ion radius (nm)	1st time	2nd time	3rd time
S1	Li^+	0.068	0.1	0.1	-
S2	Na^+	0.098	0.01	0.01	-
S3	Na^+	0.098	0.01	0.01	-
S4	Li^+	0.068	0.01	0.1	0.1
S5	Cu^{2+}	0.072	0.01	0.1	-
S6	NH_4^+	0.143	0.01	0.1	-
S7	Cu^{2+}	0.072	0.01	0.01	0.01
S8	K^+	0.133	0.01	0.01	-
S9	Li^+	0.068	0.1	-	-

2.4 Membrane permeation and separation

Single-gas permeances were measured in a dead-end, stainless steel module where one end of the membrane tube was blocked off. The permeate-side pressure was 84 kPa (atmospheric pressure in Boulder, Colorado), and the feed pressure was controlled using a pressure regulator. Before the permeance was measured, the membrane was heated to 473 K, and its feed and permeate sides were swept with the gas to be studied. Permeation rates were measured using a soap film flowmeter. The estimated permeance error was 2% for gas permeances between 10^{-5} to 10^{-9} $mol \cdot m^{-2} \cdot s^{-1} \cdot Pa^{-1}$. For gas permeances below 10^{-9} $mol \cdot m^{-2} \cdot s^{-1} \cdot Pa^{-1}$, the permeance error could be as high as 20%. The lowest measurable permeance is estimated to be 1×10^{-11} $mol \cdot m^{-2} \cdot s^{-1} \cdot Pa^{-1}$. Ideal selectivity is the ratio of single-gas permeances. The permeation of gases through zeolite membranes was sensitive to the presence water or other strongly adsorbing components. For MFI membranes, gas permeances were conducted immediately after calcination, which was used to oxidize any adsorbates. For SAPO-34 membranes, because they readily adsorb water, the membranes were stored in a 473 K oven. They were quickly removed from the oven and placed in the module under flowing gas to minimize water adsorption. The

membrane temperature dropped as much as 30 K/min during this procedure, but permeation measurements were reproducible after several repeats of this procedure.

Gas mixtures, such as H_2/CO_2, H_2/CH_4, H_2/N_2, and CO_2/CH_4, were separated in a continuous flow system. The permeate-side pressure was 84 kPa and the feed pressure was independently controlled using a back-pressure regulator; the highest feed pressure investigated was 1.7 MPa.. No sweep gas was used. Feed, retentate, and permeate flow rates were measured with a soap film flowmeter, and compositions were analyzed on-line by a HP 5890 GC (HAYSEP D_B column, Alltech) or a SRI 8610C GC (HAYSEP D column, Alltech) with a thermal conductivity detector. Log-mean partial pressure differences were used to calculate the permeances. Separation selectivity is defined as the ratio of permeances. In comparison, composition selectivity is calculated as the ratio of the quotient of the permeate mol fractions and the quotient of the feed mole fractions. To compare with polymer membranes, membrane permeability was calculated as the membrane-thickness normalized permeance.

Between 298 and 473 K, silicone or viton O-rings (McMaster Carr #203 or #110) were used to seal the membrane in the module. At high temperatures, neither silicon nor viton remain elastic. In this study, a high temperature module was designed and double cone graphite ferrules (SFDC14.7/10.7/10.2-28G, Chromalytic Technology, Australia) were used to seal the membrane at temperatures up to 773 K. Steady state separations at 473 K were compared for sealing with silicon o-rings and graphite ferrules, and the variations in the permeances and selectivities for the two arrangements were within 2%. For membrane temperatures above room temperature, the membrane module and some system lines were heated with a heating tape. For temperatures below room temperature, the module and some lines were immersed in a refrigerated ethylene glycol/water bath controlled by a chiller. The highest temperature investigated was 773 K and the lowest was 253 K.

To characterize the quality of B-ZSM-5 membranes, hexane isomers were separated by vapor permeation in a continuous flow system. A syringe pump introduced a 50/50 n-hexane/2,2-dimethylbutane (DMB) liquid feed into a preheated helium carrier flow (0.83 mL/s) where the liquid feed vaporized. The total organic feed concentration was maintained at 8%. Both sides of the membrane were at 84 kPa, and a helium sweep gas (0.83 mL/s) was used on the permeate side. Feed, retentate, and permeate flow rates were controlled with mass flow controllers and measured with soap film flowmeters, and compositions were analyzed on-line by a HP 6890 GC with a flame ionization detector and HELIFLEX AT-1 column (Alltech). Permeances and separation selectivities were calculated in the same way as for the gas mixture separation experiments.

2.5 Adsorption and crystal structure study

Zeolite crystals were either collected from the bottom of the autoclave after membrane synthesis or synthesized using the same methods as for membrane synthesis. The crystals were also post-treated using the same methods as for membrane post-treatments. Before characterization, the crystals were washed with deionized water by

repeated centrifugation, decanting, and redispersion until the pH of the upper solution was less than 8. The cleaned B-ZSM-5 crystals were calcined at 753 K for 8 h. Some calcined B-ZSM-5 crystals were silylated with methyldiethoxysilane using the same method as for B-ZSM-5 membrane silylation. The silylation procedure was also repeated once for B-ZSM-5 powder. The cleaned SAPO-34 crystals were calcined at 823 K for 8 h, and then exchanged in 0.01 M copper(II) acetate or 0.1 M lithium acetate solutions in ethanol. Ion exchange was conducted at 348 K for 4 h under reflux, and the crystals were cleaned with ethanol by repeated centrifugation, decanting, and redispersion to wash off excess acetate salts adsorbed on the crystals. They were dried in a 340 K vacuum oven for 2 h and further dried overnight at 473 K.

The crystal structure was determined by x-ray diffraction (XRD, Scintag PAD-V diffractometer) with Cu Kα radiation. The chemical composition of zeolite samples was measured by ICP (Varian UltraMass 700 inductively coupled plasma), and the standard deviation was ± 5%. Adsorption isotherms were measured in an Autosorb-1 system (Quantachrome Corp., Model As1-C-VP-RGA). Prior to each adsorption experiment, the sample was outgassed in vacuum at 493 K for about 12 h. Sample cell temperatures were controlled using water, ice-water, ethylene glyco, ethanol, n-pentane slurry, and liquid nitrogen baths. The standard deviation for adsorption loading was ± 5%. Nitrogen adsorption at 77 K was used to determine the BET surface area and the micropore volume (Dubinin-Radushkevich (DR) equation). The standard deviation for BET area and the DR micropore volume was ± 3%.

3. RESULTS AND DISCUSSION

3.1 H_2 separation through silylated B-ZSM-5 membranes

3.1.1 Effect of initial membrane quality and operating conditions

Three B-ZSM-5 membranes (B1-B3) were characterized by hexane isomer vapor separation at an n-hexane partial pressure of 3 kPa and a DMB partial pressure of 3 kPa in the feed at 473 K. These membranes were silylated with MDES and tested for H_2 separation at 523 K and a feed pressure of 222 kPa. As shown in Table 3, membranes with higher n-hexane/DMB separation selectivities before silylation had higher H_2/CO_2 separation selectivities after silylation. The H_2/CH_4 separation selectivity, however, was similar for the three silylated membranes.

Table 3 n-hexane/DMB separation selectivities before silylation and H_2 separation selectivities after silylation for three B-ZSM-5 membranes (The standard deviation of the H_2 selectivities was ~ ± 7%.)

Membrane	n-hexane/DMB separation selectivity	Selectivity after silylation	
		H_2/CO_2	H_2/CH_4
B1	120	45	41
B2	34	16	42
B3	27	10	41

The B-ZSM-5 membrane B1 was used to separate 50/50 mixtures of H_2/CO_2 and H_2/CH_4 before and after silylation at various temperatures at a feed pressure of 222 kPa. As shown in Fig. 1a, the H_2 permeance in the H_2/CH_4 mixture at low temperature decreased by almost two orders of magnitude after silylation. The H_2 permeance in the H_2/CO_2 mixture was approximately one order of magnitude lower after silylation, as shown in Fig. 1b. For clarity, the H_2 permeances in Fig. 1 were multiplied by 10 for the silylated membrane. The decrease was less for the H_2/CH_4 mixture because the H_2 permeance for the original membrane, at least at low temperature, was significantly lower when CO_2 was present than when CH_4 was present. At 473 K, the H_2 permeances in H_2/CH_4 and H_2/CO_2 mixtures were about one order of magnitude lower in the silylated membrane.

Figure 1 Hydrogen permeance before and after silylation for B-ZSM-5 membrane B1 as a function of temperature in a 50/50 mixture of (a) H_2/CH_4 and (b) H_2/CO_2. The variations in the permeances of the silylated membrane were within 2% of the values shown in this graph after it was stored in humid air for 2 months and heated at 523 K overnight.

Although the H_2 permeances decreased significantly with silylation, the permeances of the other gases decreased more, so that the H_2/CO_2 and H_2/CH_4 separation selectivities increased. The separation selectivities were more than one order of magnitude higher than the original selectivities, as shown in Fig. 2a,b. Both the H_2/CH_4 and H_2/CO_2 selectivities increased significantly as the temperature increased from 298 K to 523 K, mainly because the H_2 permeance increased with temperature. Above 573 K, H_2 permeance in the H_2/CO_2 mixture continued to increase with temperature (Fig. 2b), but the CO_2 permeance also increased, so the selectivity leveled off (Fig. 2b). The modified membranes were stable, so that when silylated membrane B1 was stored in humid air for two months at room temperature and then heated at 523 K overnight, the permeances and selectivities at 473 K for H_2/CH_4 and H_2/CO_2 mixtures were within 2% of the values in Fig. 1 and Fig. 2. The membrane also operated at 773 K in the presence of hydrogen for 16 h with no degradation.

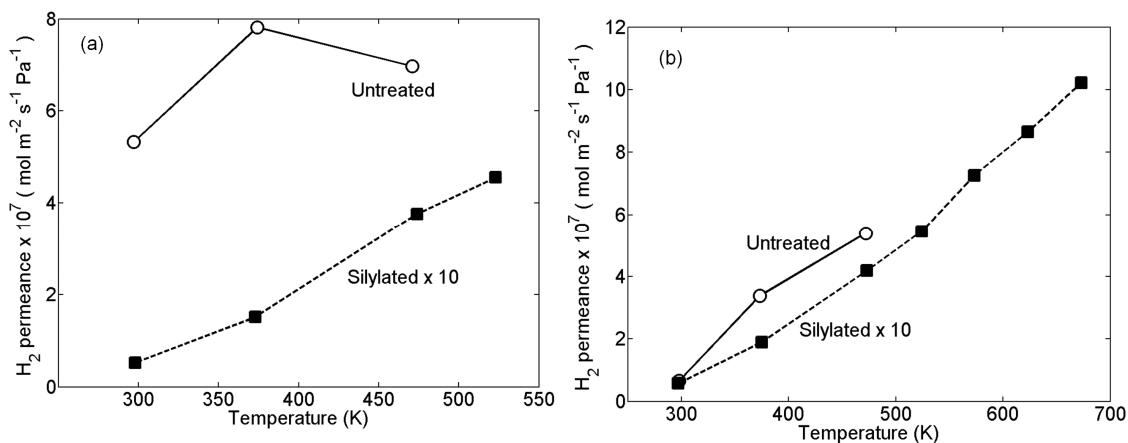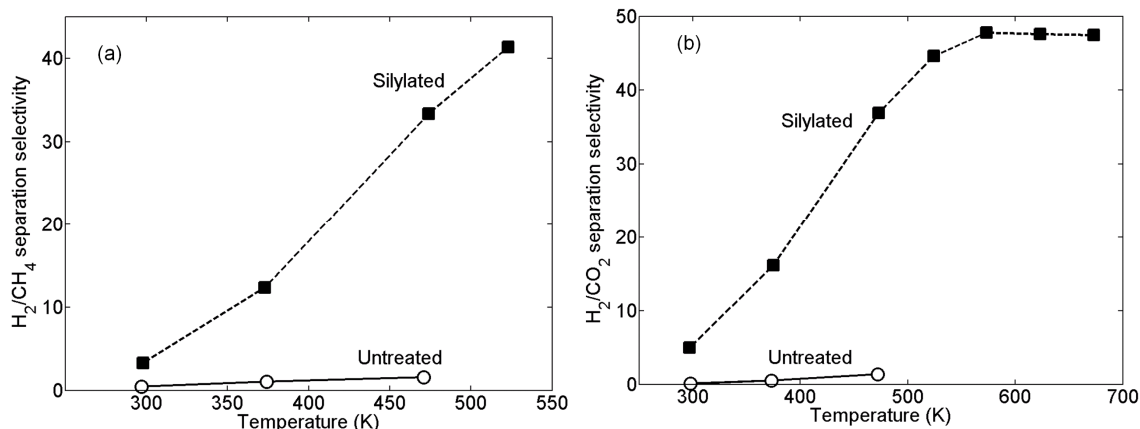Figure 2 Separation selectivity before and after silylation for B-ZSM-5 membrane B1 as a function of temperature in a 50/50 mixture of (a) H_2/CH_4 and (b) H_2/CO_2. The variations in the selectivities of the silylated membrane were within 2% of the values shown in this graph after it was stored in humid air for 2 months and heated at 523 K overnight.

Above 673 K, the H_2 and CO_2 reacted to form H_2O and CO; the modified B-ZSM-5 membrane catalyzed the reverse water gas shift reaction. Carbon monoxide was observed in the retentate and the permeate, but the GC could not detect water at low concentrations so the following concentrations are on a dry basis. At 723 K, the retentate contained 2% CO, and the CO concentration in the permeate was below 0.2%. The H_2 and CO_2 concentrations in the permeate were 93% and 7% respectively. At 773 K, the retentate contained 8% CO; the permeate contained 92% H_2, 7% CO_2, and 1% CO. Table 4 gives the percent conversion of the water-gas shift reaction, hydrogen permeances, and separation selectivities at 723 and 773 K.

Table 4 H_2 permeances and separation selectivities of silylated B-ZSM-5 membrane B1 for a H_2/CO_2 mixture at high temperature

Temperature (K)	Percent Conversion	Permeance $\times 10^8$ (mol·m^{-2}·s^{-1}·Pa^{-1})			Separation selectivity	
		H_2	CO_2	CO	H_2/CO_2	H_2/CO
723	4 %	10.5	0.23	< 0.2	46	> 48
773	15%	12.5	0.21	0.22	60	57

Silylated B1 was also used to separate H_2/N_2 at a feed pressure of 222 kPa. For the three equimolar binary mixtures, the membrane showed similar H_2 permeances and H_2 separation selectivities, as shown in Fig. 3. The H_2 permeance and the H_2 separation selectivities were almost the same for the three mixtures. The highest H_2/N_2 separation selectivity measured at 523 K was 47 with a H_2 permeance of 4.4×10^{-8} mol·m^{-2}·s^{-1}·Pa^{-1}.

16
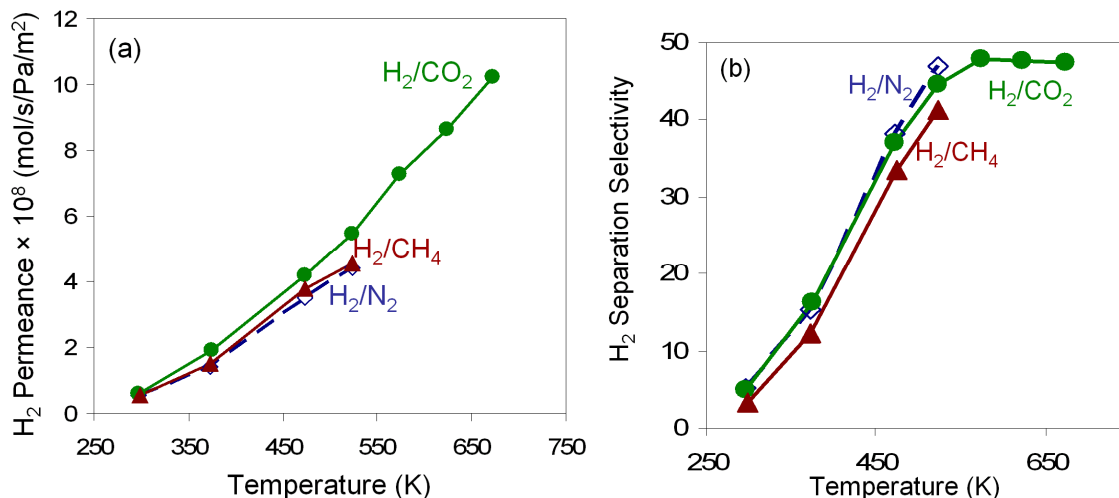
Figure 3 (a) H_2 permeances and (b) H_2 separation selectivities as a function of temperature of silylated membrane B1 for equimolar H_2/CO_2, H_2/N_2, and H_2/CH_4 mixtures at a feed pressure of 222 kPa (The standard deviation of the permeances and selectivities was ~ ± 7%.)

Robeson et al. reported upper bounds for selectivity versus permeability of polymeric membranes used for H_2/CO_2 and H_2/CH_4, and H_2/N_2 separations, and Freeman proposed a model for the upper bound observation. For H_2 separation, the upper bounds have negative slopes, reflecting the tradeoff between permeability and selectivity. In order to obtain the membrane thickness, the silylated membrane B1 was broken and Fig. 4 shows the cross-sectional view of the silylated membrane B1. The membrane was about 30 µm thick. The H_2 separation performance for the silylated B-ZSM-5 membrane B1 exceeded the upper bounds of polymer membranes (Fig. 5) when the membrane was used to separate equimolar H_2/CO_2, H_2/N_2, and H_2/CH_4 mixtures at high temperatures where polymers membranes are unstable. Note that the H_2 permeabilities were calculated based on the SEM thickness of 30 µm but the separation layer could be thicker if the B-ZSM-5 membrane grew into the support, and thus, these permeabilities for the silylated membrane B1 shown in Fig. 5 are lower limits.
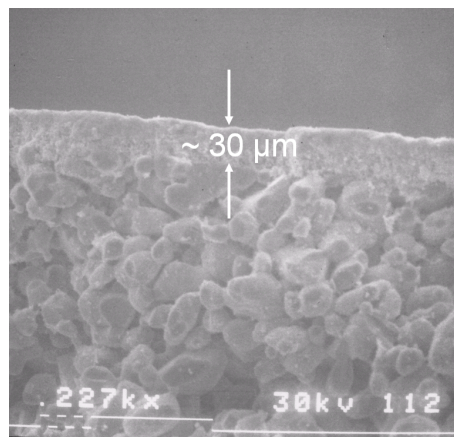
Figure 4 An SEM image of the cross section of the silylated B-ZSM-5 membrane B1
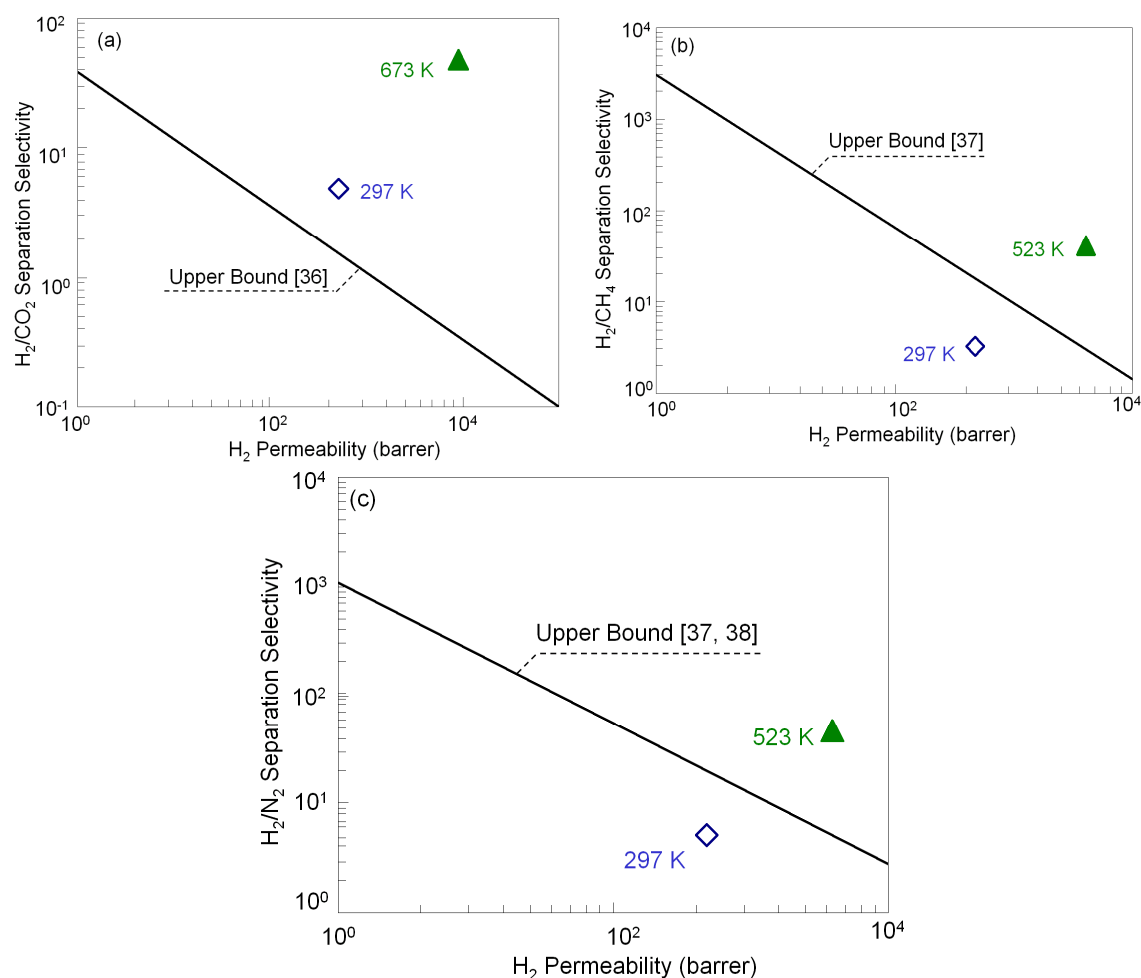
Figure 5 Separation selectivity of (a) H_2/CO_2, (b) H_2/CH_4, and (c) H_2/N_2 mixtures versus H_2 permeability for the silylated B-ZSM-5 membrane B1 at a feed pressure of 222 kPa and various temperatures. The Robeson upper bounds for polymer membranes are shown for comparison.

The single-gas fluxes of H_2, CO_2, and CH_4 through the silylated B2 increased linearly with pressure drop at all temperatures used (Fig. 6), so the permeances were almost independent of pressure drop. Hydrogen permeated faster than CO_2 and CH_4, and its permeance increased with temperature that can be fit with an Arrhenius equation, whereas CO_2 and CH_4 permeances decreased slightly with temperature. The activation energy for H_2 permeance was 8.2 kJ/mol, which is lower than the values for silica membranes of 15-38 kJ/mol.
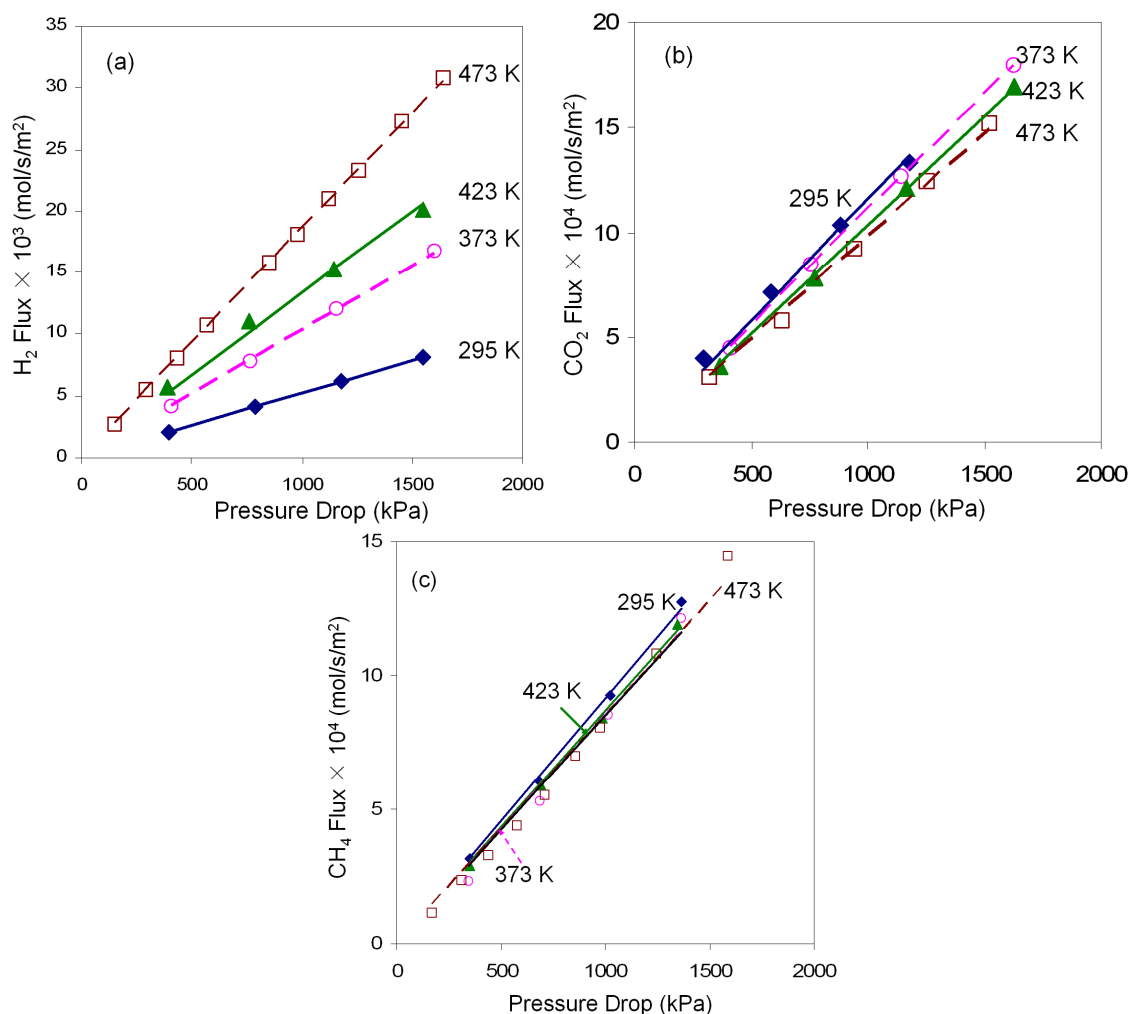
Figure 6 Single-gas fluxes for (a) H_2, (b) CO_2, and (c) CH_4 through the silylated B-ZSM-5 membrane B2 as a function of pressure drop. The lines are the linear fit of the fluxes.

The silylated membrane B2 separated H_2 from CO_2 and CH_4 at elevated pressures. Similar to previous results for a pressure drop of 138 kPa, for a pressure drop of 1.6 MPa, the H_2/CO_2 and H_2/CH_4 separation selectivity increased approximately an order of magnitude as the temperature increased from 298 to 473 K (Fig. 7). Similar to single gas, the H_2 permeances in the mixture were also activated with temperature. The activation energy for H_2 permeance was 11 kJ/mol in the mixture with CO_2 (Fig. 7a) and 13 kJ/mol in the mixture with CH_4 (Fig. 7b), slightly higher than that for single-gas H_2 permeation of 8.2 kJ/mol (Fig. 6a). The CO_2 and CH_4 permeances slightly decreased when the temperature increased, as in the gas single. The H_2 permeance in the mixture was lower than for the single gas, especially at lower temperatures. At 298 K, the H_2 permeance in CO_2 was only 42% of the corresponding single-gas permeance. The CO_2 permeance was slightly higher in the mixture than in the single gas, and the CH_4 permeance was similar in these two modes. Therefore, the ideal selectivities were higher than the mixture selectivities. The H_2/CO_2 ideal selectivity was 4.3 and 19 at 298 and 473 K, respectively, and the H_2/CH_4 ideal selectivity was 5.8 and 22.
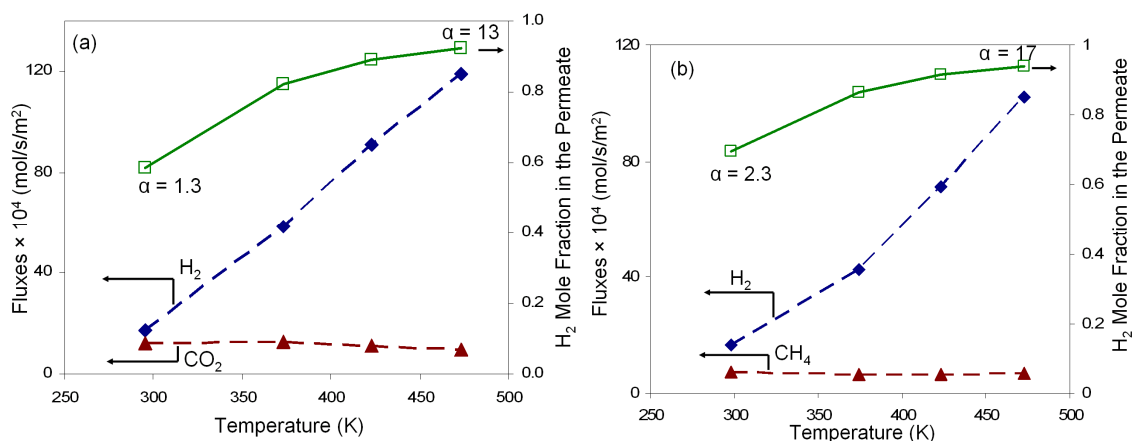
Figure 7 Fluxes and H_2 permeate mole fraction for (a) a H_2/CO_2 mixture (52/48) and (b) a H_2/CH_4 mixture (51/49) as a function of temperature through the silylated B-ZSM-5 membrane B2. The feed pressure was 1.6 MPa for the H_2/CO_2 mixture and 1.4 MPa for the H_2/CH_4 mixture.

Both H_2 and CO_2 fluxes increased as the feed pressure increased (Fig. 8a). The same behavior was observed for the H_2/CH_4 mixture (Fig. 8b). For a 51% H_2/49% CO_2 mixture, when the feed pressure increased from 0.23 to 1.6 MPa, the H_2 permeate concentration increased from 86% to 93% (Fig. 8a). Similarly, for an equimolar H_2/CH_4 mixture, when the feed pressure increased from 0.23 to 1.3 MPa, the H_2 permeance concentration increased from 90% to 94% (Fig. 8b). However, the separation selectivity calculated from the ratio of permeances did not increase. Log-mean partial pressure drop was used to calculate the permeances. The separation selectivity is the ratio of fluxes over the ratio of partial pressure drops. As the total feed pressure increased, the ratio of H_2/CO_2 or H_2/CH_4 partial pressure drops also increased. Although the ratio of H_2/CO_2 or H_2/CH_4 fluxes increased, the ratio of partial pressure drop increased proportionally more. Therefore, although the composition selectivity increased, the separation selectivity did not. Similar behavior was observed for CO_2/CH_4 separations through SAPO-34 membranes.
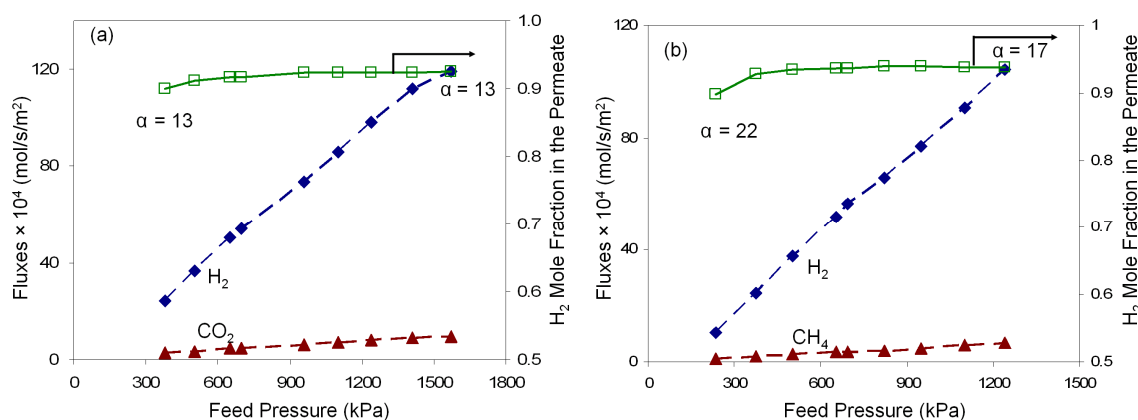
Figure 8 Fluxes and H_2 permeate mole fraction for (a) a H_2/CO_2 mixture (51/49) and (b) a H_2/CH_4 mixture (50/50) at 473 K as a function of feed pressure through the silylated B-ZSM-5 membrane B2.

20

The H_2 flux increased and the CO_2 or CH_4 fluxes decreased almost proportionally with the H_2 content in the feed (Fig. 9). The H_2 permeance in the mixture was almost constant, and the CO_2 and CH_4 permeances increased slightly when the H_2 content in the feed increased. Therefore, the separation selectivity decreased slightly as the H_2 mole fraction in the feed increased, as shown in Fig. 9.
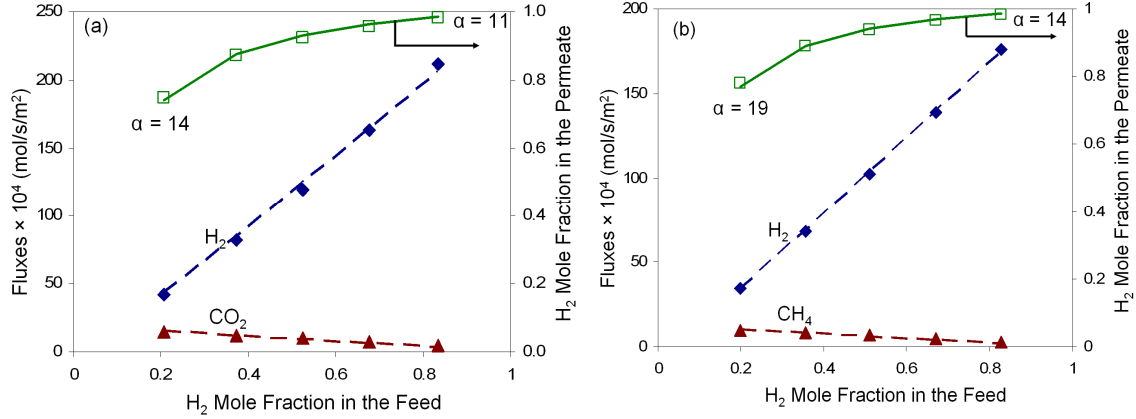
Figure 9 Fluxes and H_2 permeate mole fraction at 473 K for (a) H_2/CO_2 mixtures and (b) H_2/CH_4 mixtures as a function of H_2 mole fraction in the feed through the silylated B-ZSM-5 membrane B2. The feed pressure was 1.6 MPa for H_2/CO_2 mixtures and 1.4 MPa for H_2/CH_4 mixtures.

3.1.2 Effect of membrane acidity

To confirm that the silylation reaction using MDES takes place on the acid sites within the zeolite membranes, a B-ZSM-5 membrane with Si/B=100 (B5) and a silicalite-1 membrane (B6) were silylated using MDES. Membrane B5 has a lower concentration of acid sites than B1- B3 because less trivalent boron is present in the framework. Silicalite-1 is the all silicon analog of ZSM-5 without any active sites, since no trivalent Al or B is present in the framework. When the B-ZSM-5 membrane with a Si/B ratio of 100 (B5) was silylated, its H_2 permeance only decreased to half its initial value, and the H_2 selectivities relative to N_2, CO_2, and CH_4 only increased about 15% (Table 5). The H_2 permeance and separation selectivities of a silicalite-1 membrane (B6), which does not have acid sites, did not change after silylation (permeance and selectivity change was less than 3%). This confirms that acid sites are needed for the silylation reaction with MDES, as the MDES will be pre-adsorbed there. This is also in accordance with the literature result. Therefore, the H_2 separation performance after silylation depends on the acidity of the initial MFI membranes.

Table 5 H_2 permeances and separation selectivities at 523 K before and after silylation of a B-ZSM-5 membrane with Si/B ratio of 100 (membrane B5)

Membrane	H_2 permeance in mixture $\times 10^8$ (mol·m^{-2}·s^{-1}·Pa^{-1})			Separation selectivity		
	H_2/N_2	H_2/CO_2	H_2/CH_4	H_2/N_2	H_2/CO_2	H_2/CH_4
Fresh	27	26	29	2.0	1.7	1.4
Silylated	13	13	14	2.3	1.8	1.6

3.1.3 Effect of silane precursors

The quality of initial membrane B2 was also characterized by single-gas butane isomer permeation at 473 K and a feed pressure of 222 kPa. The membrane had an *n-/i*-butane ideal selectivity of 14 with an *n*-butane permeance of 2.4×10^{-7} mol·m^{-2}·s^{-1}·Pa^{-1}. Membrane B4 had a similar *n-/i*-butane ideal selectivity of 15 with an *n*-butane permeance of 4.6×10^{-7} mol·m^{-2}·s^{-1}·Pa^{-1}.

Membrane B4 was silylated with dilute silane and its H_2 permeance decreased more than an order of magnitude, but the H_2/CO_2 and H_2/CH_4 selectivities only increased by factors of 4-5, as shown in Table 6. Although the original C_4 isomer selectivity was similar to that of membrane B2, the H_2 permeance decreased more and the H_2 separation selectivity increased less than for membrane B2.

Table 6 H_2 permeances and separation selectivities at 473 K before and after silylation with dilute silane for B-ZSM-5 membrane B4

Membrane	H_2 permeance in mixture $\times 10^8$ (mol·m^{-2}·s^{-1}·Pa^{-1})		Separation selectivity	
	H_2/CO_2	H_2/CH_4	H_2/CO_2	H_2/CH_4
Fresh	77	96	1.1	1.1
Silylated	3.6	3.9	5.3	4.4

3.1.4 Adsorption and crystal structure study

The B-ZSM-5 crystals synthesized by secondary growth were cubic with dimensions ~ 1×1×0.2 μm. Their BET surface area was 350 m^2/g and their DR micropore volume was 0.18 mL/g, similar to Al-ZSM-5 zeolites. Silylation with MDES decreased the BET area to 310 m^2/g and the pore volume to 0.15 mL/g. Silylation did not change the CH_4 adsorption loading at 293 K and only slightly decreased the CO_2 loading (Fig. 10). At 293 K and 100 kPa, the H_2 loading was 0.08 mmol/g, which is only 10% of the CH_4 loading; this loading was too low to determine if silylation changed it. Hydrogen adsorption on the silylated powder was also measured at 77 and 160 K and its heat of adsorption was 7.4 ± 0.5 kJ/mol.
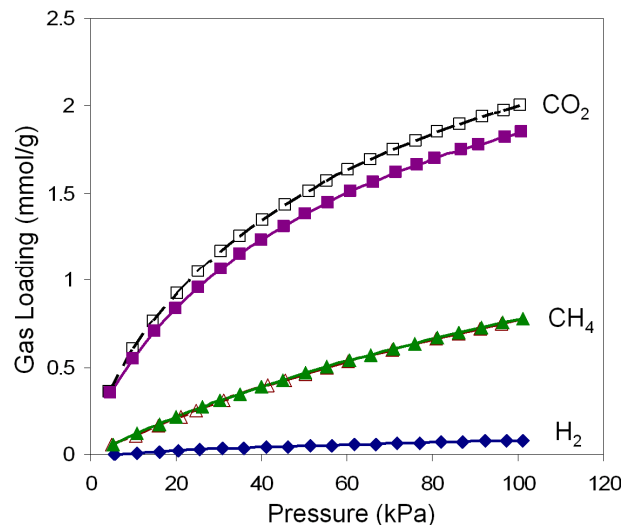
Figure 10 Adsorption isotherms of H_2, CH_4, and CO_2 at 293 K. Open symbols: original B-ZSM-5 crystals. Closed symbols: silylated B-ZSM-5 crystals

The original and silylated powders were mixed together with each kind of powder accounting for 50 wt%. The XRD pattern for the mixed powder is shown in Fig.11. The XRD pattern clearly shows split of peaks, indicating that the two kinds of powders have different zeolite pore sizes. Therefore, the XRD results confirm that MDES reacts in the zeolite pores of the MFI membrane. Since silane is smaller than MDES, it should also react in the MFI zeolite pores as well.
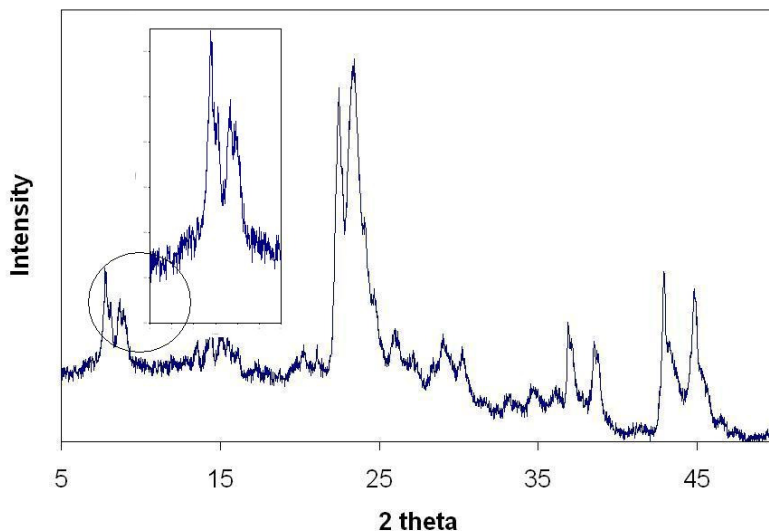
Figure 11 XRD pattern for 50/50 mixture of as-synthesized and silylated zeolite B-ZSM-5 powders (Insert: detailed XRD pattern in 2θ range between 5 and 11)

3.2 H_2 separation through SAPO-34 membranes

3.2 1 Effect of operating conditions

The CO$_2$ single-gas permeance through the SAPO-34 membrane S10 was not a strong function of temperature from 253 to 308 K, as shown in Fig. 12. The H$_2$ single-gas permeance was lower and slightly decreased when the temperature increased. Therefore, the CO$_2$/H$_2$ ideal selectivity slightly increased with temperature but the highest selectivity was only 2. The reproducibility for the single-gas permeances was about ± 7%.
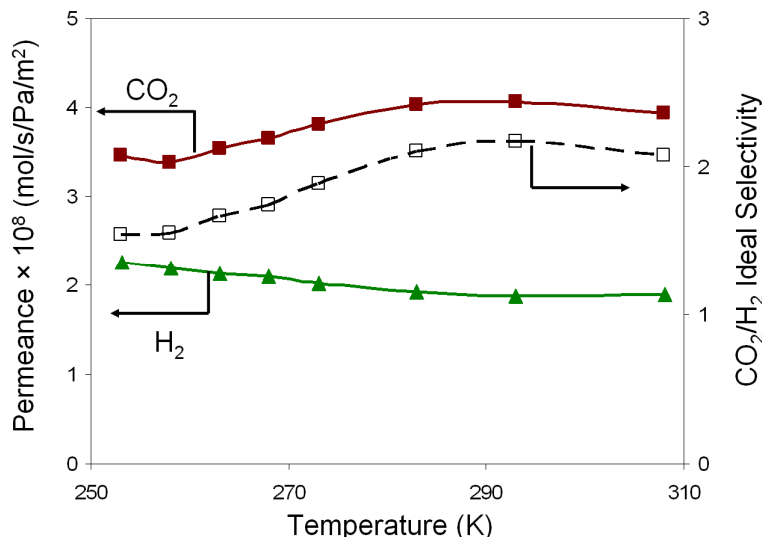
Figure 12 CO$_2$ and H$_2$ single-gas permeances as a function of temperature through the SAPO-34 membrane S10. The feed pressure was 0.6 MPa for CO$_2$ and 1.4 MPa for H$_2$.

Figure 13 shows the three repeats of binary CO$_2$/H$_2$ mixture separation. Before experiment set 1, the membrane was calcined at 633 K with a heating and cooling rate of 0.6 and 0.9 K/min respectively. The membrane was taken out of the calcination furnace at ~ 450 K and quickly mounted in the module and cooled in the chiller of 253 K. Steady state was assumed when the CO$_2$ permeance and CO$_2$/H$_2$ separation selectivity changed less than 2% in 30 min, and the values for experiment set 1 were measured by gradually increasing the membrane temperature. After experiment set 1, the membrane was taken out of the module, heated in a 523 K oven overnight without controlling the heating rate. For experiment set 2, the membrane was removed from the oven, quickly mounted in the module, and cooled in the chiller of 253 K. Then steady state CO$_2$ permeances and CO$_2$/H$_2$ separation selectivities were measured by gradually increasing the membrane temperature. When the temperature reached 308 K, the membrane was not removed from the module but stayed on the CO$_2$/H$_2$ mixture gas stream overnight and experiment set 3 was conducted by gradually decreasing the membrane temperature.

Compared with ideal selectivities, the CO$_2$/H$_2$ separation selectivities were much higher (Fig. 13b) because the H$_2$ permeance dropped orders of magnitude in the presence of CO$_2$. At 253 K, the H$_2$ permeance in the mixture was less than 1% of its single-gas permeance. On the other hand, hydrogen did not significantly affect CO$_2$ permeances. The CO$_2$ permeance in the mixture was only slightly lower than its single-gas permeance.

Note that the CO_2 single-gas permeance (Fig. 12) was measured at a feed pressure similar to the CO_2 feed partial pressure in the mixture (Fig. 13). The H_2 single-gas permeance did not depend on pressure, and thus the H_2 single-gas permeance (Fig. 12) was measured at a higher pressure than its partial pressure in the mixture (Fig. 13). The H_2 permeance in the mixture increased monotonically over an order of magnitude from 253 to 308 K. Therefore, the CO_2/H_2 separation selectivity generally decreased as the temperature increased. These CO_2 permeances and selectivities are significantly higher than those reported for polymer membranes under the same conditions. However, at 473 K, the membrane was selective for H_2 with a H_2/CO_2 selectivity of 2.
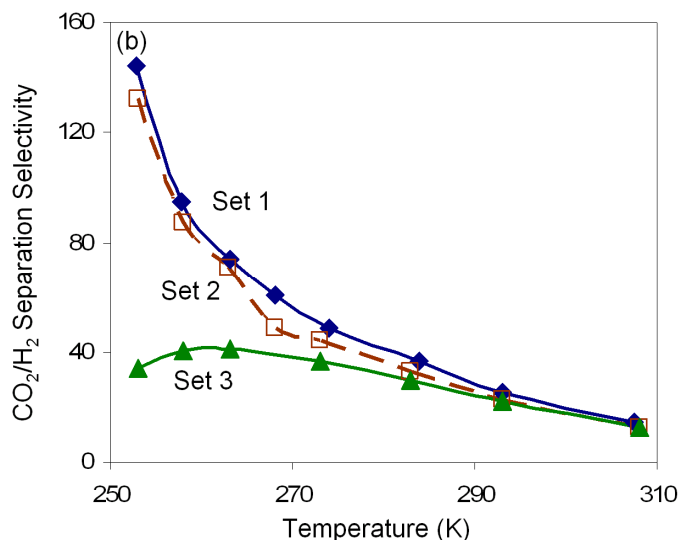
Figure 13 CO_2/H_2 separation selectivities for a CO_2/CH_4 mixture (43/57) as a function of temperature at a feed pressure of 1.6 MPa through the SAPO-34 membrane S10 from three repeated experiments

The CO_2 permeances from experiment set 2 were slightly higher than those from experiment set 1 and the CO_2/H_2 separation selectivities were slightly lower. The highest deviation of CO_2 permeance between experiment set 1 and 2 is 28%, and the highest deviation of CO_2/H_2 separation selectivity is 16%. The average deviation for CO_2 permeance and CO_2/H_2 separation selectivity is 13% and 7.7% respectively. For experiment set 2 and 3, however, the results differ significantly at low temperatures. The CO_2 permeance and CO_2/H_2 separation selectivity were 57% and 58% lower for experiment set 3 than for the experiment set 2. The CO_2/H_2 separation capacity of the SAPO-34 membrane seemed impaired by cooling the membrane slowly or keeping the membrane at longer time on stream, whereas heating it at ~ 500 K regenerated this capacity.

The effect of feed composition was investigated after the membrane was heated at 523 K overnight and cooled in the module at 253 K quickly to avoid decreasing the permeances and selectivity by cooling the membrane slowly. When the CO_2 mole fraction was increased at 253 K, the CO_2 flux increased and the H_2 flux decreased. For a pressure drop of 1.1 MPa, for 12% CO_2 in the feed, the CO_2 permeate concentration was

77%. For 43% CO_2 in the feed, the CO_2 permeate concentration was 98.8%. Increasing the feed to 78% CO_2 slightly increased the CO_2 permeate concentration to 99.6%. Therefore, the CO_2/H_2 separation selectivity exhibited a maximum of 140, as shown in Fig. 14; the corresponding composition selectivity was 110. A maximum in CO_2/H_2 separation selectivity was also seen at other feed pressures of 1.56 MPa, 0.85 MPa, and 0.45 MPa. Both CO_2 and H_2 permeances decreased with increased CO_2 feed concentration, but the H_2 permeance decreased less at high CO_2 concentrations (Fig. 14). A similar maximum in the selectivity was also observed when SAPO-34 membranes separated CO_2/CH_4 mixtures at 253 K.
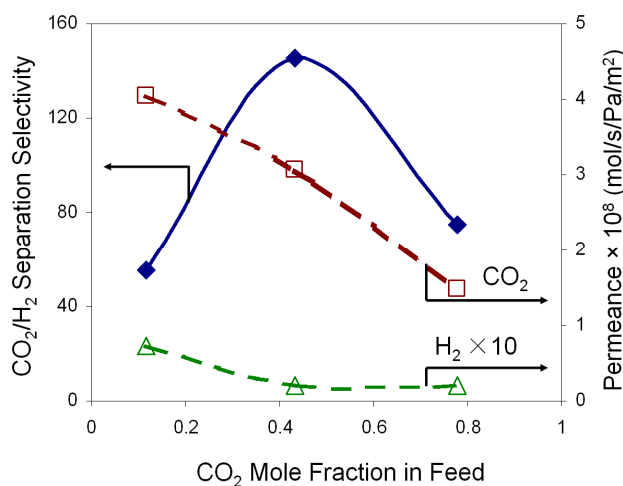
Figure 14 Permeances and selectivity at 253 K as a function of CO_2 feed mole fraction through the SAPO-34 membrane S10. The feed pressure was 1.16 MPa.

The CO_2 permeance decreased significantly at higher pressure-drop for both single gas and in mixtures with H_2 (Fig. 15). The log-mean partial pressure drop was used for mixtures so the permeances could be compared to the single-gas permeances. The data were more scattered in the mixture; the CO_2 permeances in the mixtures were measured at different feed pressures and different feed compositions (Fig.13-14). Pressure had almost no effect on H_2 permeance. The single-gas permeance of H_2 was 2.3 $\times 10^{-8}$ mol·m^{-2}·s^{-1}·Pa^{-1} at 253 K, and it changed less than 3% as the feed pressure increased from 0.23 to 1.4 MPa.
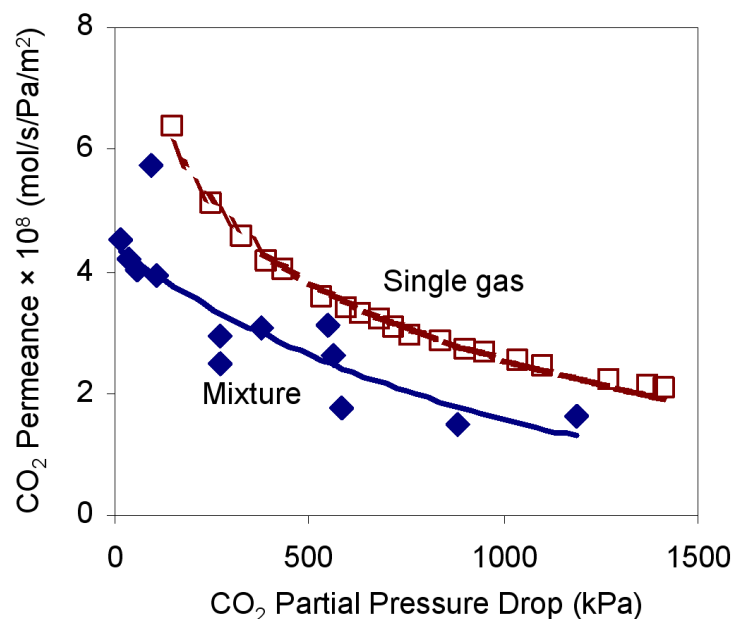
Figure 15 CO_2 permeances for single gas and in CO_2/H_2 mixtures at 253 K as a function of partial pressure drop.

3.2.2 Effect of ion exchange

The initial H-SAPO-34 crystals, synthesized from a gel with a Si/Al ratio of 0.3, had a unit cell (u.c.) composition of $|H^+_{2.8}|[Si_{3.9}Al_{17.4}P_{14.7}O_{72}]$, corresponding to a Si/Al ratio of 0.22, as measured by ICP. The H and O content was added based on an idealized SAPO-34 framework structure and charge balance. The acid site density, calculated based on 2.8 H^+ ions per unit cell and a unit cell mass of ~ 2200 atomic weight, was ~1.3 mmol/g. Each unit cell of SAPO-34 has 3 CHA cages, and approximately one cation resides in each CHA cage. About 22% of the H^+ sites exchanged with Cu^{2+} after exposure to 0.01 M $CuAc_2$, and almost 100% of the H^+ sites exchanged with Li^+ after exposure to 0.1 M LiAc.

As shown in Fig. 16, when SAPO crystals were exchanged with Cu^{2+} ions and washed once, copper acetate salts were detected by XRD. These salts were completely removed after 3 washings. The XRD powder patterns of SAPO-34 did not change after exchange with Cu^{2+} or Li^+ ions and complete washing. For H-SAPO and completely-washed Cu-SAPO and Li-SAPO, the XRD patterns match the intensities and line positions reported for SAPO-34, and indicate a single SAPO-34 phase; exchange did not degrade the crystals.
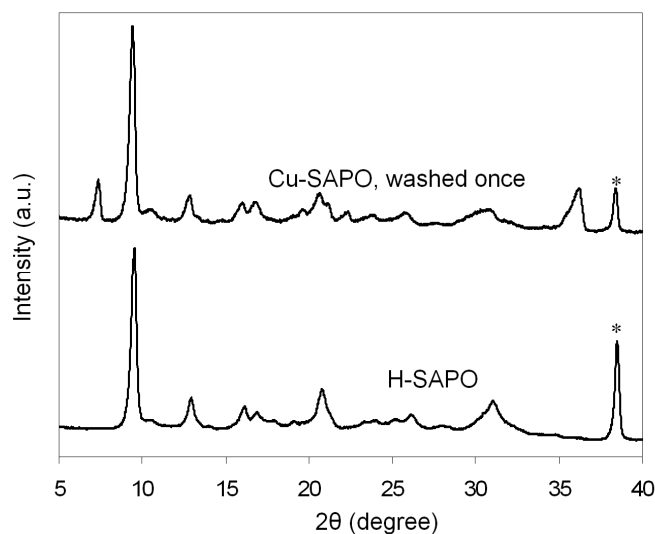
Figure 16 XRD patterns of SAPO-34 crystals; the asterisk denotes peaks from the supporting aluminum plate

Nitrogen adsorption isotherms were used to determine the surface area and the pore volume of SAPO-34 crystals before and after exchange. As shown in Table 7, the BET surface area for H-SAPO crystals was 490 m^2/g and its DR micropore volume was 0.26 mL/g. Copper exchange had almost no effect on the BET surface area and micropore volume, whereas Li^+ exchange decreased those values by approximately 15%. Note, however, that only 22% of the sites exchanged with copper (II). Cu^{2+} exchange had almost no effect on saturation loadings, whereas Li^+ exchange decreased the CO_2 and CH_4 saturation loading by about 14%. The q_{sat} values for H-SAPO are higher than we previously estimated from isotherms at 253 K. Saturation loadings should be relatively temperature independent, but estimates can be low when using isotherms that are not at low enough temperature to be close to saturation.

Table 7 Adsorption properties of SAPO-34 crystals

Sample		H-SAPO	Cu-SAPO	Li-SAPO
Degree of exchange (%)		-	22	100
BET surface area (m^2/g)		490	490	420
Micropore volume (cm^3/g)		0.26	0.26	0.22
q_{sat} (mmol/g)	CH_4 143 K	6.1	6.3	5.3
	N_2 77 K	7.6	7.6	6.4
q_{sat} (molec./u. c.)	CH_4 143 K	13	14	12
	N_2 77 K	17	17	14

The H_2, CO_2, and CH_4 single gas permeances decreased after ion exchange, as shown in Fig. 17 for Li^+ exchange (membrane S9), and the percent decrease was higher for CH_4 (48% at 295) than for H_2 or CO_2 (25% - 30% at 295 K). The single gas permeances of H_2 and CO_2 decreased with temperature, whereas the CH_4 permeance was relatively independent of temperature. Similar behavior was observed for Na^+-, NH_4^+-, and Cu^{2+}-exchanged membranes. At 295 K, CO_2 (0.33 nm kinetic diameter) permeated faster than H_2 (0.29 nm), but CO_2 permeance decreased more with temperature so that at

473 K, H_2 permeated faster. Methane (0.38 nm) permeated significantly slower than H_2 or CO_2, and thus its permeances are multiplied by 10 in Fig. 17.
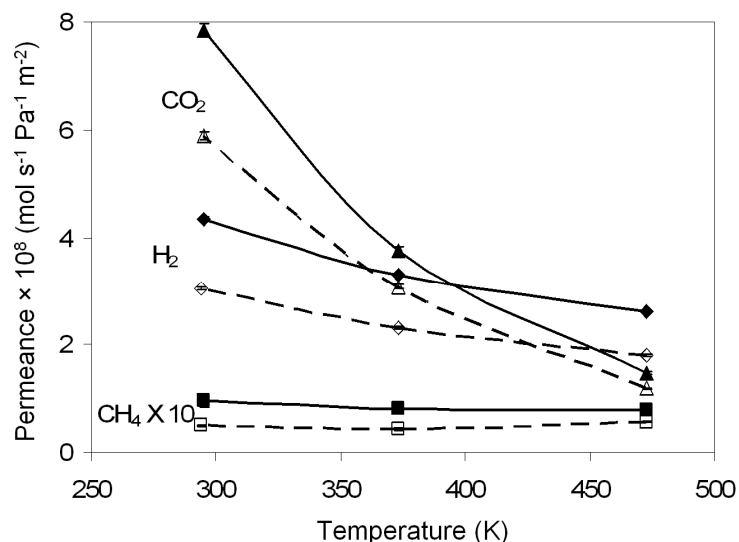
Figure 17. Temperature dependencies of single gas permeances for membrane S9 before (solid line) and after (dashed line) Li^+ exchange (The standard deviation of the single-gas permeances was ~ $\pm$ 7%)

The H_2/CH_4 and CO_2/CH_4 ideal selectivities increased after Li^+ exchange, as shown in Fig 18 for membrane S9. The selectivities decreased with temperature. Similar behavior was observed for Na^+-, NH_4^+-, and Cu^{2+}-exchanged membranes, and Table 8 compares the CO_2 permeances and ideal selectivities before and after the first ion exchange.

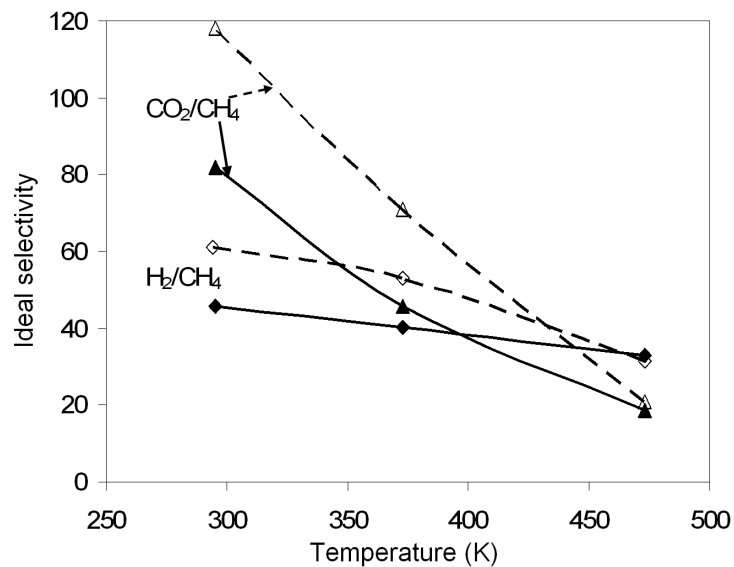Figure 18. Temperature dependencies of H_2/CH_4 and CO_2/CH_4 ideal selectivities for membrane S9 before (solid line) and after (dashed line) Li^+ exchange (The standard deviation of the ideal selectivities was ~ ± 7%)

Table 8 Single gas CO_2 permeances and ideal selectivities for SAPO-34 membranes

#	Ion[*]	T (K)	CO_2 permeance× 10^8 (mol·m^{-2}·s^{-1}·Pa^{-1})		Ideal selectivity			
					H_2/CH_4		CO_2/CH_4	
			Original	Changed	Original	Changed	Original	Changed
S2	Na^+	295	5.6	5.1	21	27	36	46
		473	0.97	0.81	16	20	8.2	8.8
S3	Na^+	295	6.4	5.7	20	22	32	36
		473	1.2	1.1	12	13	5.6	6.3
S4	Li^+	295	6.1	5.0	23	26	37	45
		473	1.1	0.85	17	20	7.9	9.6
S5	Cu^{2+}	295	4.6	3.9	25	28	46	54
		473	0.65	0.38	18	19	6.4	7.9
S6	NH_4^+	295	7.1	5.8	19	29	31	47
		473	1.3	1.2	16	18	8.5	11
S9	Li^+	295	7.8	5.9	46	61	82	118
		473	1.5	1.2	32	32	19	21

[*] Ion exchange was conducted only once

Ion exchange decreased H_2 permeances for a 50/50 H_2/CH_4 feed, but the H_2/CH_4 separation selectivity was essentially unchanged, as shown in Fig. 19 for Li^+ exchange on membrane S4. The H_2/CH_4 separation selectivities are lower than the ideal selectivities shown in Table 8. The H_2 permeances slightly decreased as temperature was increased from 297 to 473 K, and the H_2/CH_4 separation selectivity did not change significantly. Similar behavior was also observed for Na^+-, K^+-, NH_4^+-, and Cu^{2+}-exchanged membranes, and Table 9 compares the H_2 separation performance for other membranes before and after ion exchange. The largest decrease in H_2 permeance was for the biggest cations. The H_2 permeance through membrane S6 decreased 61% after NH_4^+ exchange, and it decreased 37% through membrane S8 after K^+ exchange, whereas other ions decreased the H_2 permeance less than 20%. The H_2/CH_4 separation selectivity generally increased less than 10%, which is close to the reproducibility (~ 7%). The highest percent increase (18%) was for Cu^{2+} exchange, the H_2/CH_4 selectivity increased from 16 to 19 at 473 K for membrane S7. The highest H_2/CH_4 separation selectivity at 473 K was for membrane S9, which was 32 in its original H^+-form and 35 after Li^+ exchange.
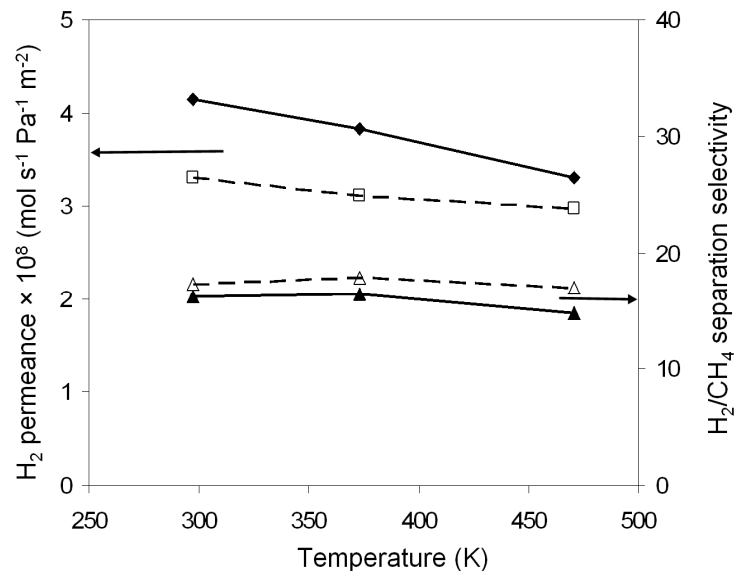
Figure 19 Temperature dependencies of H_2 permeance and H_2/CH_4 separation selectivity for membrane S4 before (solid line) and after (dashed line) Li^+ exchange

Table 9 H_2 permeance and H_2/CH_4 selectivity of 50/50 mixtures of SAPO-34 membranes before and after the first ion exchange at 473 K and 138 kPa pressure drop

No.	Ion[*]	H_2 permeance[**]		H_2/CH_4 separation selectivity	
		Original	Exchanged	Original	Exchanged
S1	Li^+	33	29	17	18
S2	Na^+	30	26	15	16
S3	Na^+	41	34	14	14
S5	Cu^{2+}	24	21	16	17
S6	NH_4^+	45	28	14	15
S7	Cu^{2+}	34	31	16	19
S8	K^+	28	21	18	15
S9	Li^+	37	28	32	35

* The ion exchange procedure was conducted only once.
** Permeances in the unit of ($\times 10^{-9}$ mol·m^{-2}·s^{-1}·Pa^{-1})

Interestingly, ion exchange increased CO_2/CH_4 separation selectivities significantly and decreased CO_2 permeances, as shown in Table 10. Repeating the exchange using the same or higher ion concentration (Table 2) had almost no effect, except for K^+ and NH_4^+, the largest cations. The CO_2 permeance decreased and selectivity increased after the second K^+ exchange. For NH_4^+ exchange, the permeance decreased and selectivity increased after the first exchange (0.01 M), but the second exchange (0.1 M) decreased selectivity below that of the original membrane and reduced CO_2 permeance by more than 50%.

Table 10 CO_2 permeances and CO_2/CH_4 separation selectivities at 295 K for SAPO-34 membranes

Membrane	Ion	CO$_2$ mixture permeance $\times 10^8$ (mol·m^{-2}·s^{-1}·Pa^{-1})			CO$_2$/CH$_4$ separation selectivity		
		Original	First	Second	Original	First	Second
S1	Li$^+$	11	8.0	8.0	66	86	87
S2	Na$^+$	8.8	7.4	7.4	59	73	75
S3	Na$^+$	12	7.6	7.7	64	66	70
S4	Li$^+$	10	7.0	7.0	60	76	77
S5	Cu^{2+}	8.4	5.2	5.2	64	74	81
S6	NH$_4^+$	13	7.6	3.6	55	72	48
S7	Cu^{2+}	8.9	-	7.8	49	-	69
S8	K$^+$	10	7.3	5.1	40	55	64
S9	Li$^+$	11	6.3	-	136	144	-

3.2.3 Effect of Silylation

Two SAPO-34 membranes (S11, S12) with similar properties were prepared; their gas permeances and selectivities are shown in Table 11. The untreated SAPO-34 membrane S11 selectively separated H$_2$ from CH$_4$ (Fig. 20); the highest selectivity was 35, measured at 298 K. The H$_2$/CH$_4$ separation selectivity was high for the original SAPO-34 membranes because the SAPO-34 pores are almost the same size as the CH$_4$ kinetic diameter, which is 0.38 nm, and CH$_4$ diffusion through SAPO-34 pores is restricted. In contrast to B-ZSM-5 membranes, silylation did not decrease H$_2$ permeances in mixtures for SAPO-34 membranes (Fig. 21 and Table 11). The CH$_4$ permeance decreased after silylation (Fig. 21), so that the H$_2$/CH$_4$ selectivity increased (Fig. 20). For clarity, the CH$_4$ permeance in Fig. 21 is multiplied by 20. The highest H$_2$/CH$_4$ separation selectivity for the silylated SAPO-34 membrane S1 was 59 at 298 K. As temperature increased, the H$_2$ permeance slightly decreased and the CH$_4$ permeance slightly increased, so the H$_2$/CH$_4$ separation selectivity decreased with temperature. The CH$_4$ permeance increased more for the silylated membrane. Thus, as shown in Fig. 20 and 21, at 525 K, silylation had no effect on permeance or selectivity. Silylation also increased the CO$_2$/CH$_4$ separation selectivity at room temperature, as shown in Table 11. The CO$_2$ permeance in a CO$_2$/CH$_4$ mixture decreased about 30% due to silylation.

Table 11 Gas permeances and separation selectivities at 298 K on SAPO-34 membranes before and after silylation

	Membrane	H$_2$ permeance $\times 10^8$ (mol·m^{-2}·s^{-1}·Pa^{-1})	H$_2$/CH$_4$ selectivity	CO$_2$ permeance $\times 10^8$ (mol·m^{-2}·s^{-1}·Pa^{-1})	CO$_2$/CH$_4$ selectivity
S11	Fresh	4.7	35	10	73
	Silylated	4.8	59	7.7	110
S12	Fresh	3.4	20	10	68
	Silylated	3.5	30	6.4	87

Figure 20 H_2/CH_4 separation selectivity before and after silylation for SAPO-34 membrane S11 as a function of temperature in a 50/50 mixture of H_2/CH_4. The standard deviation of the permeances was $\sim \pm 7\%$.
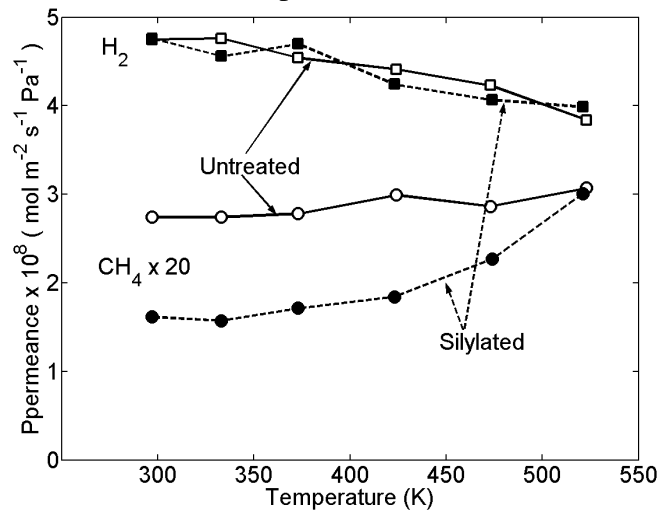
Figure 21 H_2 and CH_4 permeances before and after silylation for SAPO-34 membrane S11 as a function of temperature in a 50/50 mixture of H_2/CH_4. The standard deviation of the selectivities was $\sim \pm 7\%$.

The SAPO-34 membranes had much lower selectivities for H_2/CO_2 and H_2/N_2 mixtures than for H_2/CH_4 mixtures, but the selectivities increased with temperature, as shown in Fig. 22. Silylation did not change the H_2/CO_2 separation selectivity, and it increased the H_2/N_2 separation selectivity by less than 15%. Similar to the H_2 permeance in the H_2/CH_4 mixture, the H_2 permeances in H_2/CO_2 and H_2/N_2 mixtures did not change after silylation. Similar H_2/CH_4 and H_2/CO_2 separation performance with temperature (not shown here) was seen for membrane S12 before and after silylation.
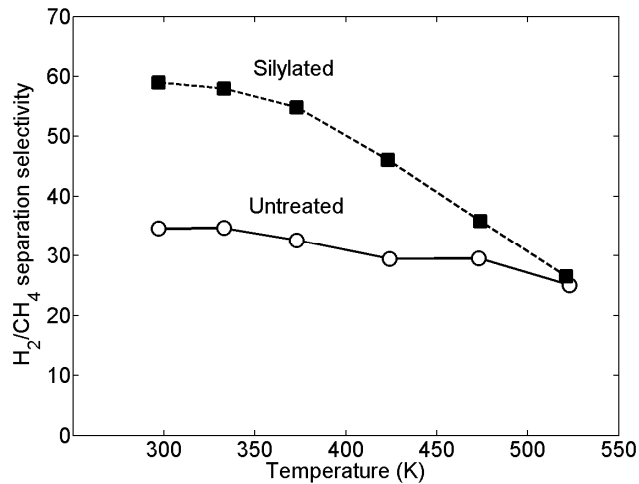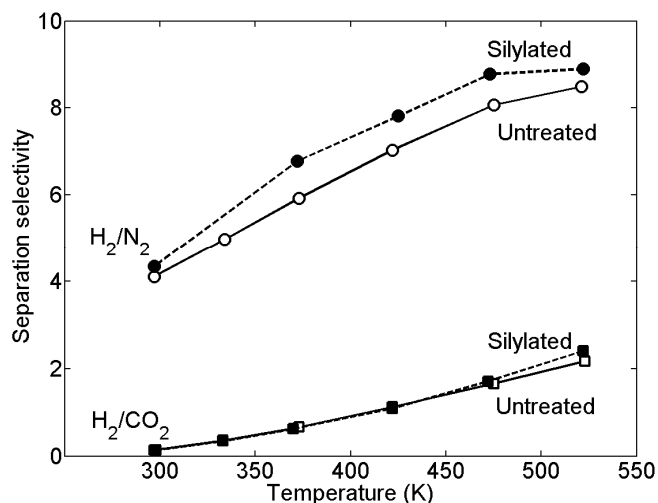
33

Figure 22 Separation selectivity before and after silylation for SAPO-34 membrane S11
as a function of temperature in 50/50 mixture of H_2/CO_2 and H_2/N_2

4. CONCLUSIONS

Zeolite membranes were prepared onto porous tubular stainless steel or α-alumina supports by *in-situ* crystallization or secondary growth from various gels. These membranes had either a medium-pore-MFI-type structure (B-ZSM-5) or a small-pore-CHA-type structure (SAPO-34).

The as-synthesized zeolite membranes were modified by silylation or ion exchange to improve their gas separation performance. Boron-substituted ZSM-5 and SAPO-34 membranes were silylated by catalytic cracking of methyldiethoxysilane (MDES) on acid sites to increase their selectivity for H_2 separation from light gases. Silylation on B-ZSM-5 crystals decreased their pore volume, but had almost no effect on the CO_2 and CH_4 adsorption. The increase in the H_2 separation selectivity was mainly due to the increase in diffusion differences. Silylation decreased the effective zeolite pore size of B-ZSM-5 membranes and increased their H_2 separation selectivities. For example, the H_2/CO_2 separation selectivity at 473 K increased from 1.4 to 37, whereas the H_2/CH_4 separation selectivity increased from 1.6 to 33 for a B-ZSM-5 membrane. However, H_2 permeance decreased more than an order of magnitude. Both the H_2 permeance and H_2/CO_2 and H_2/CH_4 separation selectivities significantly increased with temperature up to 773 K. The highest H_2/CO_2 and H_2/CH_4 separation selectivities were 48 and 41, respectively. The highest H_2 permeance during separations was 1×10^{-7} mol·m^{-2}·s^{-1}·Pa^{-1}. The H_2 separation performance of the silylated B-ZSM-5 membranes depended on the initial membrane quality and acidity. For SAPO-34 membranes, methyldiethoxysilane did not fit into zeolite pores, but silylation apparently decreased the pore size of non-zeolite pores in SAPO-34 membranes. After silylation, H_2 permeances and H_2/CO_2 and H_2/N_2 separation selectivities were almost unchanged in SAPO-34 membranes because H_2, CO_2, and N_2 permeate mainly through SAPO-34 pores. In contrast, H_2/CH_4 separation selectivity increased from 35 to 59, and CO_2/CH_4 separation selectivity

increased from 73 to 110, apparently because some CH_4 permeates through non-SAPO-34 pores.

H-SAPO-34 zeolite membranes were exchanged with Li^+, Na^+, K^+, NH_4^+, and Cu^{2+} cations in an effort to improve their gas separation performance. Ion exchange conducted in non-aqueous solutions changed the diffusion and adsorption properties of SAPO-34 zeolites without damaging the crystal structure and membrane integrity. Ideal and separation selectivities for H_2/CH_4 mixtures increased less than 18%, whereas ideal and separation selectivities for CO_2/CH_4 mixtures increased up to 60% due to ion exchange of zeolite membranes. The H_2, CO_2, and CH_4 permeances decreased through SAPO-34 membranes upon exchange, and the decrease was larger for large cations such as K^+ and NH_4^+, apparently due to steric hindrance. Multiple exchanges did not degrade SAPO-34 crystals or membranes.

The effect of temperature, pressure, and feed composition on H_2/CO_2 and H_2/CH_4 separation through a SAPO-34 membrane and a silylated B-ZSM-5 membrane was investigated. The SAPO-34 membrane had a strong adsorption of CO_2 and thus at 253 K, it selectively separated CO_2 over H_2 with selectivity over 100. The CO_2/H_2 selectivity exhibited a maximum with CO_2 feed concentration and decreased with the membrane temperature. Although CH_4 adsorbed more strongly than H_2, the SAPO-34 membrane separated H_2/CH_4 because CH_4 diffusion was restricted in SAPO-34 pores; the separation selectivity was only slightly affected by feed composition, temperature, and feed pressure. For a silylated B-ZSM-5 membrane, both the H_2 flux and the H_2 permeate concentration increased with membrane temperature and feed pressure. The SAPO-34 membrane and the silylated B-ZSM-5 membrane had higher fluxes and composition selectivities at higher pressures. Both membranes exceeded the upper bounds of polymer membranes.

5. RECOMMENDATIONS FOR FUTURE WORK

Boron-substituted ZSM-5 membranes have been shown to have higher selectivities than other isomorphously substituted (Al, Ge, Si, and Fe) MFI membranes synthesized by *in-situ* crystallization. This research study used a secondary growth method for synthesizing B-ZSM-5 membranes and used the membranes for silylation. The seeding method used was conventional dip coating with ~ 80 nm spherical seeds. Better seeding techniques, such as electrostatic attraction and covalent linkage exhibit better seed coverage, even with bigger seeds, which are better for crystal intergrowth. An additional mesoporous silica layer before seeding may also be applied to improve support smoothness and avoid zeolite penetration into the support. Such a layer can also reduce aluminum leaching from the support and reduce stress-induced crack formation during the calcination step. Bigger seeds, better seeding techniques, and an additional silica layer between membrane and support have produced better silicalite-1 membranes. They should also lead to better B-ZSM-5 membranes than those obtained in this report. Silylation on those better membranes should yield higher H_2 permeance and H_2/light gas selectivities.

The silylated MFI membranes were catalytically reactive at high temperatures, and one membrane catalyzed water gas shift reaction. The membranes separated H_2 at temperature up to 773 K and at pressures up to 1.7 MPa. Most membranes lose selectivities at high temperatures (e.g. 500-900 K) where reactions may take place. Therefore, the silylated MFI membranes are ideal candidates for membrane reactor applications, combining reaction and H_2 separation into one unit. Membrane reactors are compact and could save energy costs if separations were done at elevated process temperatures, this research study has shown that zeolite membranes can be used at high temperature and membrane modules can be sealed at these temperatures.

This project study focused on H_2 purification (H_2/CO_2 and H_2/CH_4) and CO_2 removal (CO_2/CH_4) with silylated MFI and SAPO-34 membranes. Other commercially important gas separations are also possible through those membranes, including H_2/N_2 separation related to ammonium purge gas preparation, N_2/CH_4 separation related to nitrogen removal from natural gas, and CO_2/N_2 separation relevant to CO_2 capture from flue gas. For silylated MFI membranes, binary mixtures of H_2/N_2 were separated with fluxes and selectivities close to those of H_2/CO_2 and H_2/CH_4. A more detailed study on this separation is desirable. Only binary mixtures were studied in this thesis and separations at more realistic conditions should be conducted. These conditions include separating a feed mimicking dry syngas (30 vol% H_2, 30 % CO, 25 % CO_4, and 15 % CH_4) at temperatures up to 900 K and high feed pressures.

For ion exchanged SAPO-34 membranes, studying CO_2/N_2 separation is recommended. For a H-SAPO-34 membrane with a CO_2/CH_4 selectivity of ~100 at room temperature, its CO_2/N_2 selectivity was only ~ 20. Nitrogen (0.364 nm) is slightly smaller than the SAPO-34 pore size (0.38 nm), whereas CH_4 (0.38 nm) is close to the SAPO pore size, and N_2 diffusivity is expected to be higher than CH_4 diffusivity. This thesis has shown that ion exchange increased CO_2 adsorption strength and/or decreased SAPO-34 pore volume in some cases, and these changes increased CO_2/CH_4 separation selectivity. The decrease in the SAPO-34 pore volume might reduce the effective pore size of the SAPO-34 membranes. This might in turn lead to a significant decrease in the N_2 diffusivity as N_2 might be excluded from the slightly decreased pores. Therefore, ion exchange is expected to increase CO_2/N_2 mixture selectivity more than CO_2/CH_4 selectivity as a large fraction of CH_4 flow was already through the non-zeolite pores before ion exchange. Similar to CO_2/CH_4 and CO_2/H_2 separation, the CO_2/N_2 selectivity should increase when the temperature decreases and the temperature effect should be explored.